HORIBA Scientific

200 YEARS 1819-2019 HORIBA JOBIN YVON

AFM-Raman

TERS Characterization of Single- to Few-Layer $Ti_3C_2T_x$ MXene

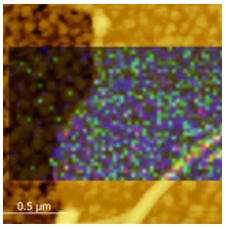

Application Note

TERS-MXenes AFM24

A. Sarycheva[1], M. Shanmugasundaram[2], A. Krayev[2], Y. Gogotsi[1], A. Tempez[3], M. Chaigneau[3]

[1]A. J. Drexel Nanomaterials Institute and Department of Materials Science and Engineering, Drexel University, Philadelphia, Pennsylvania 19104, United States, [2]HORIBA Scientific, Piscataway, New Jersey 08854, United States,[3]HORIBA FRANCE SAS, Palaiseau, France

Abstract: This application note reports on TERS characterization of $Ti_3C_2T_x$ MXene flakes. MXenes are a large 2D materials family gaining interest for their high electronic conductivity and hydrophilic surface. Nano-resolved chemical imaging of single-layer and few-layer flakes of $Ti_3C_2T_x$ MXene deposited on a gold substrate has been realized at a laser power density on the sample about an order of magnitude lower as compared to confocal Raman measurements. Spectra feature an intense peak at around 201 cm^{-1} and two well-defined peaks at around 126 and 725 cm^{-1}. While the intensities of these peaks decrease with increasing number of layers, the relative intensity of the 126 and 725 cm^{-1} bands as compared to the 201 cm^{-1} band increases. The peak positions of the main MXene bands do not significantly change in flakes of different number of layers, suggesting weak coupling between the MXene layers. This note also shows that TERS signal can be used to monitor the onset of degradation of single- and few-layer flakes of $Ti_3C_2T_x$ well before significant morphological changes appear and thereby assess their environmental stability.

Keywords: TERS, Raman spectroscopy, MXenes, two-dimensional materials, plasmonics, interface, vibrational properties.

Context and Issues

MXenes are a growing 2D materials family with a $M_nX_{n-1}T_x$ general formula, where M is a transition metal, X is C and/or N, and T_x stands for the functionalization group (O, OH, F, Cl, etc.) resulting from their wet-chemical synthesis. They have unique properties such as high electronic conductivity and a hydrophilic redox-active surface [1-3]. Some Mxene compounds exhibiting semiconducting properties have been theoretically predicted [4].

MXenes' properties may be tuned by varying the transition metal [5], the number of layers (n) [6], and the surface terminations [7]. The influence of the stoichiometric ratio on the properties is known for some systems but the effects of local heterogeneities still need to be investigated. The control of nanoscale composition would ultimately allow for engineering properties locally, gaining more control over the 2D material-based systems.

Potential / Input from technique

Raman spectroscopy provides valuable information about the structural properties of such materials [8-9] but Raman microscopy fails to image chemical nano-heterogeneities due to the optical diffraction limit. Furthermore, in the case of MXene, the conventional Raman signal is very weak and the integration time required to collect a decent S/N spectrum is tens of seconds at the laser power level still not damaging for the sample, which makes the imaging de-facto prohibitive. Tip-enhanced Raman spectroscopy (TERS) overcomes the low Raman signal level by enhancing Raman scattering up to 6 orders of magnitude and enables nanoscale chemical mapping [10].

Starting point, what is known?

TERS achievements in establishing structure–property relationships in 2D materials on a nanometer scale are now well documented [11]: characterization of local defects, strain, and Moiré pattern in graphene [12], doping and nanoscale strain-related structural heterogeneities [13] which affect their optoelectronic properties in a large number of transition metal dichalcogenides (TMDCs).

In this application note, we report on TERS measurements carried out on monolayer to few-layer thick $Ti_3C_2T_x$ and Ti_3C_2 flakes. The reader may refer to the article by Sarycheva *et.al* in ACS Nano: Tip-Enhanced Raman Scattering Imaging of Single- to Few-Layer $Ti_3C_2T_x$ MXene [14].

Description of sample and measurements

MXene crystals were synthesized using the method described in [15] and then deposited on gold substrates. The gold substrate permits the so-called gap mode TERS conditions,

in which an optical electric field is greatly amplified in the cavity created by the apex of the TERS tip and plasmonic gold surface.

AFM and TERS measurements were performed using a nanoRaman system (XploRANano, HORIBA Scientific) integrating an atomic force microscope (SmartSPM) and a Raman microscope (XploRA) with a 100× WD objective tilted by 65° with respect to the sample plane for excitation and collection. 785 or 830 nm excitation *p*-polarized lasers were focused onto the cantilever-based gold coated AFM-TERS tip (OMNI-TERS-SNC-Au, Applied Nanostructures Inc.). The power on the sample was about 350 µW for 785 nm excitation and about 450 µW for 830 nm. It should be also noted that the far-field (confocal µRaman) signal from the $Ti_3C_2T_x$ crystals was negligible at the laser power level and integration times used in TERS experiments, especially for the mono-, bi- and tri-layer thick flakes. The maps were acquired in SpecTop or Dual Two Pass modes. While both modes imply direct contact with the sample for recording strong TERS signal, in the SpecTop mode, transition between the pixels of the TERS map is performed in alternating-contact mode. Fig. 1 displays a schematic diagram of the TERS experiments and Raman-active vibrations of $Ti_3C_2T_x$ MXene.

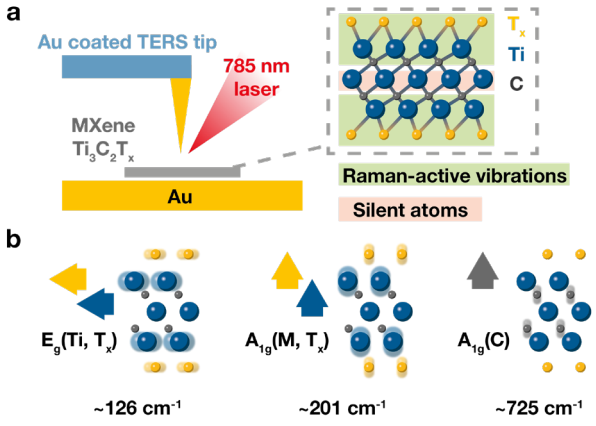

Figure 1: (a) TERS schematic diagram and $Ti_3C_2T_x$ atomic crystal arrangement; (b) Raman active vibrations of $Ti_3C_2T_x$ discussed in this work: in-plane E_g vibration at 126 cm^{-1} mainly appears when the excitation wavelength matches the surface plasmon resonance of $Ti_3C_2T_x$, and out-of-plane vibrations at 201 and 725 cm^{-1} correspond to vibrations of Ti, C, T_x, and C, respectively.

Fig. 2a shows a topographic image of several MXene flakes on gold substrate. The height profile inset in Fig. 2a goes across a monolayer (1L), bilayer (2L), and a small overlap between the two. A TERS map collected over these flakes with 785 nm excitation is presented in Fig. 2c. It shows the distribution of the intensity of three main $Ti_3C_2T_x$ Raman peaks: ~126 cm^{-1} band, a resonant Raman band, also described as E_g vibration of Ti, C, and T_x groups (green color), 201 cm^{-1} band, which corresponds to A_{1g} (Ti, C and T_x) vibration (blue color) and another resonant Raman band at 725 cm^{-1} which corresponds to A_{1g} (C) vibration (red color).

The change of absolute and relative intensities of major Raman bands as a function of layer thickness can be observed by looking at average spectra of typical flake areas plotted in Fig. 2b. The absolute intensities of all three major bands at 126, 201, and 725 cm^{-1} are highest for the monolayer flake and decrease with the number of layers because of lower coupling between the tip and the substrate. The out-of-plane A_{1g} (Ti, C, T_x) is the most enhanced peak in the monolayer flake which is expected as this vibration is aligned with the laser optical electric field of the band-gap mode tip-substrate cavity. The other out -of-plane A_{1g} (C) mode is less enhanced.

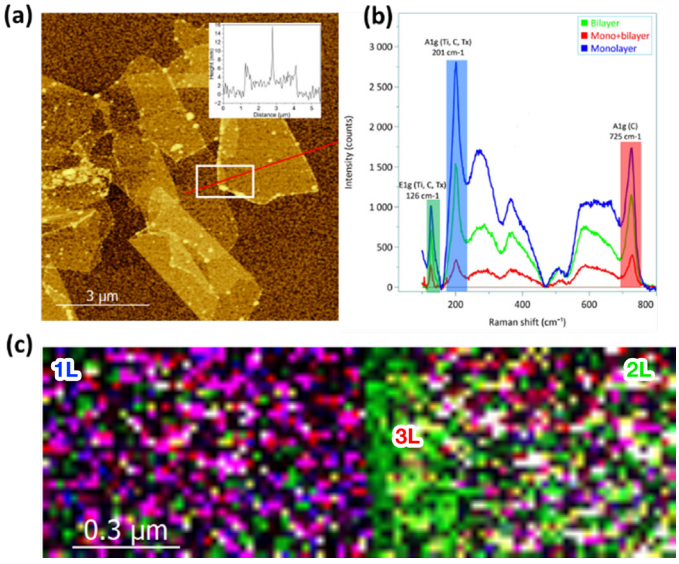

Figure 2: (a) Topographic AFM image of several $Ti_3C_2T_x$ flakes on Au substrate. The white dashed rectangle indicates the TERS scan area (c); Inset: Height profile along the line showing that there are slightly overlapping single-layer and bilayer crystals; (b) TERS spectra averaged over the monolayer (blue spectrum), bilayer (green spectrum), and trilayer regions (bilayer overlapped with the monolayer, orange spectrum). The background was subtracted and spectra were offset vertically for clarity. (c) 1.8 µm × 0.6 µm, 90 pixels/line TERS map showing the distribution of the intensity of correspondingly colored bands.

In the deposition process of single- to few-layer thick MXene flakes from aqueous solution, some folds and nanowrinkles form when the flakes get attached to the substrate. A topographic image of a 5 nm thick (trilayer) $Ti_3C_2T_x$ flake with such wrinkles crossing the flat flake surface is presented in Fig. 3a. The height profile across the line shows that the wrinkles were about 5–10 nm high. A combined TERS map (Fig. 3c) collected at 785 nm laser excitation shows the intensity distribution of the three same $Ti_3C_2T_x$ Raman peaks as in Fig. 2c: ~126 cm^{-1} band (green color), 201 cm^{-1} band (blue color),

and 725 cm^{-1} band (red color). TERS spectra plotted in Fig. 3d shows the contrast between the dominant out-of-plane A_{1g} (Ti,C,T_x) vibration in the flat area and the dominance of the two resonant A_{1g} (C) and E_g vibrations over the wrinkles. In addition, it should be noted that the main A_{1g} (Ti,C,T_x) peak shifts from 201 to 202–203 cm^{-1} over the wrinkles. From previous studies in graphene and graphene oxide deposited on gold, nanoscale wrinkles may feature increased TERS response due to improved coupling of the in-plain carbon modes (D, G, and 2D) to the optical field in the tip–sample gap in vertical walls of the wrinkles [16]. In our case, we observe simultaneous enhancement of both the in-plane E_g mode at 126 cm^{-1} and the out-of-plane A_{1g} (C) mode at 725 cm^{-1}, which indicates that the TERS enhancement mechanism in the case of the wrinkles in MXenes is different from the one observed in graphene and graphene oxide. It has been reported earlier that MXenes with their metallic nature may support surface plasmon resonances in the visible and near-infrared range. The transversal surface plasmon resonance being around 780 nm, the resonant Raman conditions in $Ti_3C_2T_x$ are met when using the 785 nm excitation. The mechanical deformation at the wrinkles may induce sharper or more intense plasmonic resonance (versus the adjacent flat material) and results in enhanced intensities of the two resonant 126 and 725 cm^{-1} modes. Comparison with TERS map (data not shown here) collected at 830 nm displaying lower (three times in peak height) intensity of the 725 cm^{-1} band further confirms the resonance effect observed at 785 nm.

An improved synthetic method can produce flakes with highly stoichiometric Ti_3C_2 composition. Fig. 4a shows an example of these flakes and one can notice the cleanliness of the edges compared to the TiO_2 particles surrounding the edges of the above studied $Ti_3C_2T_x$ flakes. This is due to removal of salts through rinsing. In addition, such "cleaner" flakes feature longer lasting TERS signal. The batches that did not undergo thorough rinsing lost TERS activity within about a week in ambient after deposition, way before significant morphological changes occurred in the deposited flakes which makes TERS a useful tool for monitoring the early stages of Ti_3C_2 degradation The stability of the cleaned MXene samples has thus been examined by collecting AFM topography images and TERS spectra from the same group of monolayer flakes every 10 days for 2 months.

The sample was stored in a glass Petri dish under ambient conditions (~21°C), without direct exposure to the sunlight. As we can see from Fig. 4a–d, after two months in ambient, a slightly elevated (about 1 nm or less) borderline of the crystals was found, indicating potential oxidation and/or hydrolysis along the edges due to the exposure to ambient oxygen and humidity. Nonetheless, the monolayer crystals are still clearly visible, their morphology did not change, and all main Raman features are observed in their TERS spectrum (Fig. 4d).

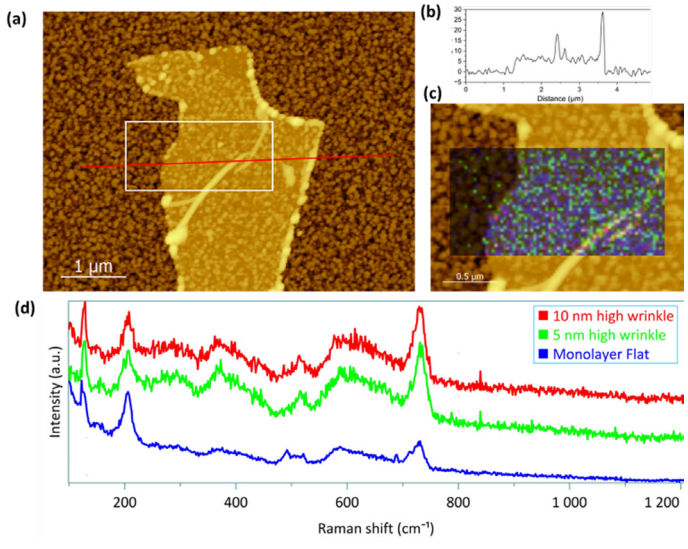

Figure 3: (a) Topographic AFM image of a tri-layer (5 nm-thick) $Ti_3C_2T_x$ crystal on gold substrate. Two wrinkles of 5 and 10 nm in height can be seen in this topography image. Increased height at the edges of the flake could come from the formation of titania nanoparticles as a result of MXene degradation; (b) AFM trace along the line shown in panel a; (c) combined 2 µm × 1 µm, 72 pixels per line TERS map showing the distribution of the intensity of 126 cm^{-1} (green color), 201 cm^{-1} (blue color), and 725 cm^{-1} (red color) peaks overlaid over the topography image. (d) TERS spectra averaged over the flat part of the crystal (blue spectrum), large 10 nm wrinkle (black spectrum), and small 5 nm wrinkle (gray spectrum). Spectra were offset vertically for better visualization.

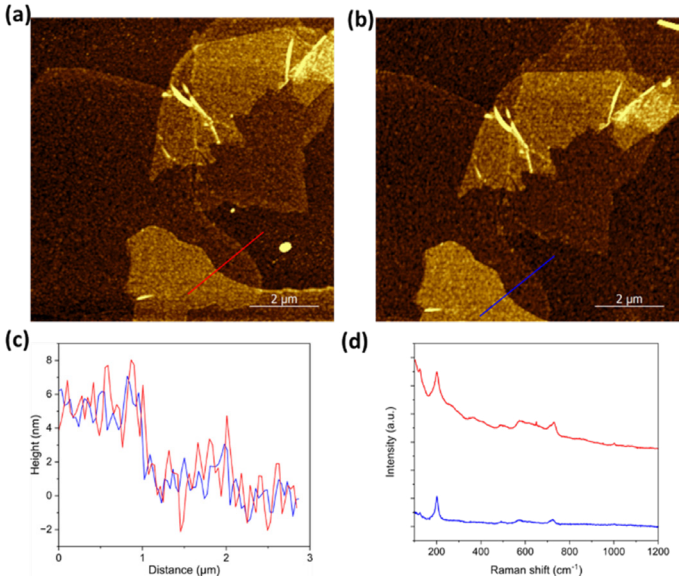

Figure 4: (a,b) Topographic images and corresponding AFM line scans of the same area taken immediately after deposition and (c) after 2 months of storage. (d) TERS spectra averaged over several locations on the monolayer flakes taken right after deposition (blue spectrum) and after 2 months of storage (red spectrum). The TERS activity of the monolayers was preserved after two months under ambient conditions and no significant morphological changes in the crystals were found. Difference in the background intensity of TERS spectra is due to varying plasmonic response of the TERS probes utilized for the corresponding measurements over an extended period of time.

Conclusions and perspectives

This note shows that TERS can be used to image with nanoresolution single- to few-layer thick flakes of $Ti_3C_2T_x$ MXene deposited on gold substrate.

It is observed that the relative intensity of the E_g peak at 126 cm^{-1} and A_{1g} (C) peak at 725 cm^{-1} as compared to the intensity of the 201 cm^{-1} peak increases with thickness. This observation can be used to differentiate monolayers from the few-layer thick flakes based on their TERS spectra. Special TERS response from nanowrinkles in $Ti_3C_2T_x$ was observed: both the absolute and relative intensities of 126 and 725 cm^{-1} bands were increased as compared to the adjacent flat area. Finally, we showed that the intensity of the TERS signal from the MXene crystals can be used for monitoring the early stages of degradation in ambient conditions.

References

1. M. Naguib, V.N. Mochalin, M. W. Barsoum, and Y. Gogotsi, Y. Adv. Mater. 26, 992–1005 (2014).
2. A. Bhat, S. Anwer, K.S. Bhat, et al., npj 2D Mater Appl 5, 61 (2021).
3. Anasori, B., Lukatskaya, M. R. & Gogotsi, Y. Nat Rev Mater 2, 16098 (2017).
4. XH. Zha, Q. Huang, J. He, et al. Sci Rep 6, 27971 (2016).
5. M. Han, K. Maleski, C. E. Shuck, et al., J. Am. Chem. Soc., 142, 19110–19118 (2020).
6. B. Anasori, C. Shi, E.J. Moon et al., Nanoscale Horiz., 1, 227–234 (2016).
7. J. L Hart, K. Hantanasirisakul, A. C. Lang, et al., Nat. Commun., 10, 522 (2019).
8. P.-H. Tan, Raman spectroscopy of Two-Dimensional Materials, Springer Series in Materials Science, vol 276, Singapore (2019).
9. A. Sarycheva, Y. Gogotsi, Chem. Mater., 32, 3480–3488 (2020).
10. N. Kumar, B.M., Weckhuysen, A.J.., Wain, et al., Nat Protoc 14, 1169–1193 (2019).
11. References in Correlated TERS, TEPL and SPM measurements of 2D materials HORIBA application note (2020)
12. Gadelha, A.C., Ohlberg, D.A.A., Rabelo, C. et al., Nature 590, 405–409 (2021).
13. T. P. Darlington, C. Carmesin, M. Florian, et al., Nat. Nanotechnol., 15, 854–860 (2020).
14. A. Sarycheva, M. Shanmugasundaram, A. Krayev, and Y. Gogotsi, ACS Nano, 16, 4, 6858–6865 (2022).
15. T. S. Mathis, K. Maleski, A. Goad et al., ACS Nano, 15, 6420–6429 (2021).
16. A. Bhattarai, A. Krayev, A. Termiyazev, et al., Nano Lett., 18, 4029–4033 (2018).

info.sci@horiba.com
www.horiba.com/scientific

USA:	+1 732 494 8660	**France:**	+33 (0)1 69 74 72 00	**Germany:**	+49 (0) 6251 8475 0
UK:	+44 (0)1604 542 500	**Italy:**	+39 06 51 59 22 1	**Japan:**	+81(75)313-8121
China:	+86 (0)21 6289 6060	**India:**	+91 (80) 4127 3637	**Singapore:**	+65 (6) 745-8300
Taiwan:	+886 3 5600606	**Brazil:**	+55 (0)11 2923 5400	**Other:**	+33 (0)1 69 74 72 00